04

An investigation of the diode properties of a double layer of a combined gas discharge

© B.M. Brzhozovskii,[1] M.B. Brovkova,[1] S.G. Gestrin,[2] E.P. Zinina,[1] V.V. Martynov[1]

[1] Blagonravov Institute of Machine Science, Russian Academy of Sciences,
Moscow, Russia
[2] Gagarin Saratov State Technical University,
410054 Saratov, Russia
e-mail: gestrin.s@yandex.ru

The paper shows that upon ignition of the combined gas discharge in the resonator chamber, there appears a double layer with diode properties that consists of layers of positive and negative charges surrounding the workpiece. An increase in the level of microwave power supplied to the chamber leads to a decrease in the equivalent diode resistance in open and closed modes and an increase in the current flowing through the unit. The ions of the process gas (nitrogen or argon) ionized by the microwave field fall on the product surface and diffuse into it as a result of the thermal diffusion process, which hardens the surface layer. The product is heated when a positive bias potential is applied to it by a stream of high-energy electrons arriving at the surface and accelerated to energies of tens and hundreds eV in the discharge acceleration zone. Ion-plasma implantation leads to a significant increase in the strength, wear resistance and corrosion resistance of the surface of the processed product.

Keywords: microwave gas discharge, diode effect, layered structure of the discharge, hardening of the surface layer of metal products, ion-plasma diffusion implantation, current-voltage characteristics, processing unit equivalent circuit.

Introduction

The current picture of the development of global industrial production shows that the problem of increasing the durability of metal products for various purposes continues to remain relevant.

The problem of life time increasing is solved through strengthening treatment of the surface layer of workpieces [1–3]. Well-known methods of plasma hardening treatment include: thermal hardening [4–6], ion-plasma diffusion implantation [7–9], ion-beam hardening treatment [10,11], MPACVD method (Microwave Plasma Assisted CVD) deposition of polycrystalline diamond films [12–14], allowing to change the properties of the surface layer and facilitating increasing of itshardness.

Ion-plasma diffusion saturation of the surface layer of the workpiece with nitrogen is called nitriding. The treated part, which is under a negative potential $\sim 0.4-1.1$ kV, is immersed in a low-pressure glow discharge plasma in a gas containing nitrogen. Positively charged atomic nitrogen ions are accelerated in the cathode layer towards the part. During bombardment, ions are implanted into the surface, heating it to a temperature $500-600°$C and higher, which ensures thermal diffusion of the saturating element in the part volume.

For chemical-thermal treatment of materials in plasma, not only gas discharges can be effectively used, but also low-energy electron beams that create plasma with an energy flux density of $1-10$ W/cm^2 [15–17].

A large number of experimental and theoretical works relate to the consideration of the effects of glow and microwave gas discharges on the surface of workpieces [18–31]. Thus, the papers [30,31] discuss the treatment of workpieces placed near the antenna — cathode inside a resonator chamber filled with argon at a pressure $P = 40-130$ Pa, in a cloud of superdense plasma $\omega_P = \sqrt{n_e e^2/\varepsilon_0 m_e} > \omega$, where e — elementary electric charge, m_e — electron mass, $\omega = 1.54 \cdot 10^{10}$ s^{-1} — oscillation frequency of microwave field created by the magnetron.

This area of studies also includes papers [26–29], that studied the surface hardening of treated metal samples under the effect of low-temperature plasma of an asymmetric combined gas discharge in a process unit developed by the authors.

Samples and workpieces made of structural and alloy steels (45. ShKh-15, Kh16N3MAD, 40Kh, 12Kh13, 40Kh13, 12Kh18N10T, Kh12MF, R6M5, R18), as well as alloys (brass, D16T), including hard (tungsten and titanium-tungsten-cobalt).

In the resonator chamber of the unit there was a weakly ionized process gas (nitrogen, argon, or a mixture of them) at a pressure $P = 200-400$ Pa under the simultaneous effect of microwave field created by a magnetron with an operating cyclic frequency $\omega = 1.54 \cdot 10^{10}$ s^{-1}, and a

constant electric field that occurs when a constant positive bias potential $\varphi_0 \approx 50-250$ V is applied to the workpiece. A plasma discharge cloud was formed near the workpiece surface. The treatment method proposed in [26–29] makes it possible to focus microwave energy directly on the workpiece, and in this it differs significantly from the approach developed in [30,31]. The microwave power usually used for treatment, amounting to $P_0 \approx 30-150$ W, came from the magnetron along a ring waveguide through slits into the resonator chamber. In [27,29] it was shown that the combined discharge has a layered structure and consists of a near-surface layer, a zone of electron acceleration to high energies $\sim 50-200$ eV, a zone of electron deceleration and a zone of ambipolar diffusion of electrons with ions to the walls of the resonator chamber.

This paper shows that the acceleration zone, which acquires a positive charge due to the fast electrons exit from it, and the negatively charged deceleration zone form a double layer with diode properties. The „diode" resistance in closed operation mode is by $100-1000$ times greater than its resistance in open mode $R_{back} \gg R_{forw}$. The low throughput capacity of the „diode" in the closed mode is associated with the presence of a negative floating potential $-U_f$ on the workpiece, which leads to the existence in the near-surface layer of the discharge of a potential barrier eU_f that does not allow electrons with energy $\varepsilon_e \leq eU_f$ to approach the surface, while electrons with energy $\varepsilon_e > eU_f$ create a negative current $I_e = 0.1-10$ mA, compensating the current of positive ions. In this case, the high-energy electrons formed in the acceleration zone, accelerated by the microwave field, move freely to the chamber walls, creating a diffusion current $I_e = 0.1-2$ A and losing energy in the deceleration zone, the energy is spent for excitation and ionization of molecules or atoms of process gas located there. Therefore, in the deceleration zone the final dissipation of the main portion of the microwave power supplied from the magnetron occurs.

When a positive bias potential φ_0 is applied to the workpiece, the height of the potential barrier decreases, and the electron current directed to the surface increases, reaching values $I_e = 2-20$ mA exceeding the ion saturation current $I_e > I_{i0}$. By changing the value of the bias potential, you can control the height of the potential barrier for electrons, and thereby the resistance of the „diode" in closed mode R_{back}.

A decrease in R_{back} leads to an increase in the supply of high-energy electrons from the acceleration zone to the surface of the workpiece, and thereby to increase in the temperature of the workpiece to the values $500-600°$C and higher (up to the melting point) required for thermal diffusion of ions in the part volume.

Thus, the method discussed in this paper can be considered a type of ion-plasma diffusion implantation, when a combined gas discharge is used instead of a glow discharge, and the workpiece surface is heated not due to accelerated ions, but due to a flow of high-energy electrons.

The novelty of the proposed hardening approach lies in the possibility of treating workpieces with complex surface relief without the use of scanning devices and low microwave discharge powers — $0.03-0.3$ kW, which is achieved due to the discharge localization on the workpiece itself. In this case, the maximum growth rate of the thickness of the hardening layer $0.4\,\mu$m/min is achieved in areas of the surface with maximum positive curvature. When treating metal-cutting tools such as a milling cutter, drill, or cutter, maximum surface hardening occurs near their cutting edges. A detailed comparison of the capabilities of the technology proposed by the authors for applying the hardening layer with the capabilities of applying diamond coatings using modern MPACVD methods is carried out in Section 3.

The main results of the effect of combined gas discharge plasma on the surface layer of the workpiece are changes in morphology and chemical composition. The microhardness and density of the layer increase, and its electrical and thermal conductivity decrease. A decrease in thermal conductivity is of great importance for metal-cutting tools for various purposes, for example, solid and prefabricated cutters, since the input of excess heat into it leads to intensification of the processes of material creep, and, as a consequence, an increase in the rate of defects (crater and wear chamfer) formation, leading to loss of operability.

The action on the plasma surface layer of combined discharge leads to a significant change in its properties [29]: strength increasing in terms of microhardness on average by 1.5 times; wear resistance by $2-3$ times, corrosion resistance by $2-6$ times and, as a result, increase in the life time of workpieces.

The objectives of this paper are:

1) Study of the diode properties of the double layer formed near the surface of the workpiece, formed by the acceleration zone and the deceleration zone of the discharge, determination of their dependence on the level of microwave power supplied to the chamber, as well as the possibility of these properties control by applying the constant bias potential to the workpiece φ_0;

2) study of the processes occurring in a process unit based on the analysis of its equivalent scheme with lumped parameters;

3) finding optimal conditions for the workpiece treatment for further improvement of the life time.

1. Equipment, methods and approaches

1.1. Brief description of process unit

The process of low-temperature plasma modification is implemented in a special unit, which includes (Fig. 1):

— vacuum system and process gas injection system, creating a low-pressure environment in the working chamber (~ 300 Pa), in which ionization processes continuously occur;
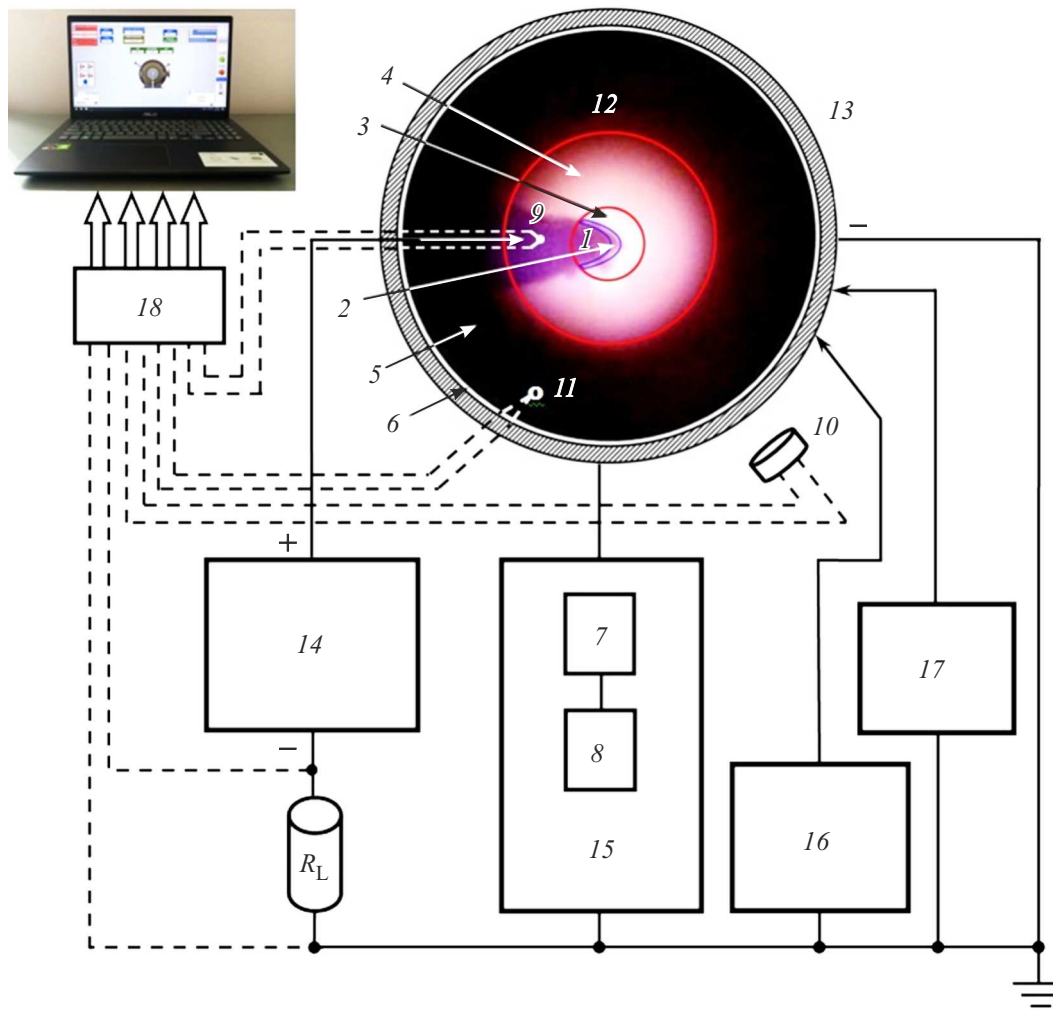
Figure 1. Scheme of the unit and process of low-temperature plasma modification: *1* — workpiece, *2* — near-surface layer, *3* — zone of electron acceleration, *4* — zone of electron deceleration, *5* — ambipolar diffusion zone, *6* — cathode layer, *7* — magnetron, *8* — autonomous filament transformer, *9* — thermocouple, *10* — photodiode, *11* — vacuum meter, *12* — discharge, *13* — working chamber, *14* — constant voltage source, *15* — microwave energy generator, *16* — vacuum system, *17* — gas injection system, *18* — analog-to-digital converter, R_L — load resistance.

— microwave energy generator and constant voltage source, forming ultra-high-frequency electromagnetic and electrostatic fields in the working chamber, the interaction of which ensures the ignition of plasma discharge directly around the workpiece surface and the energy transfer to it by plasma electrons and ions.

To monitor the discharge effect on the workpiece surface, feedback channels are implemented in the unit control system, through which signals are transmitted about the bias current, the temperature at the workpiece end not directly exposed to the plasma (lag temperature), the intensity of the discharge glow and the pressure in the working chamber. These signals are registered using a voltmeter, a thermocouple, a photodiode and a filled-system transducer, which display the parameters of electrical, thermal and optical processes (Fig. 1).

A cylindrical resonator chamber of the unit with an internal radius of walls $r_{wall} = 7.5$ cm and length $l = 30$ cm has frequencies of natural vibration of the form E_{mnp}:

$$\omega_{mnp} = c \sqrt{\left(\frac{v_{mn}}{r_{wall}}\right)^2 + \left(\frac{p\pi}{l}\right)^2}, \qquad (1)$$

where v_{mn} — root with number m of the Bessel function of order n. Substituting into (1) $v_{11} = 3.832$, as well as the dimensions of the resonator chamber, we find $\omega_{110} = 1.53 \cdot 10^{10}\,\mathrm{s^{-1}}$ for the mode E_{110}, which is close to the cyclic frequency of the magnetron $\omega = 1.54 \cdot 10^{10}\,\mathrm{s^{-1}}$.

1.2. Equivalent scheme of unit and determination of its lumped parameters

The equivalent scheme of the work unit is shown in Fig. 2. Let us determine the values of the main parameters

of its elements. Section *1–2* represents the magnetron, characterized by power P_0 and frequency ω. Circuit *3–6* limits the equivalent scheme of the resonator chamber with the fundamental oscillation E_{110}, C, L, G_{wall} — capacitance, inductance, and active conductivity of the walls, respectively. C_1 and C_2 — mutual capacitances of the workpiece and the walls of the resonator chamber. When the discharge occurs in the resonator chamber, a diode effect appears, accompanied by the appearance of a double layer consisting of layers of positive and negative charges surrounding the workpiece (electron acceleration and deceleration zones, respectively). In the open mode, the „diode" lets in fast electrons from the acceleration zone to the deceleration zone and has a relatively low resistance R_{forw}.

The decrease in fast electrons in this region is constantly replenished due to the acceleration of slow electrons in the high-frequency electric field of the microwave discharge. In the closed mode (workpiece potential $\Delta\varphi > -U_f$), the resistance of the „diode" R_{back} is high and a small electron current flows through the „diode" slightly exceeding the ionic saturation current $|i_e| > i_{i\_\text{satur}}$.

If we draw an analogy between the double layer and the vacuum diode, then the acceleration zone plays the role of a cathode, and the electrons accelerated in it to high energies are similar to the electrons leaving the cathode due to thermionic emission. Sections *6–7* and *5–9* contain the diode *VD*, corresponding to the double layer of gas discharge, the diode resistances in open and closed modes are R_{forw} and R_{back}.

The scheme section *8–10* contains a constant voltage source, the EMF of which is ε, and internal resistance $r = 1\,\text{k}\Omega$, load resistance R_L and a voltmeter V. The source is necessary to supply a constant bias potential to the workpiece ε_0. If $\varepsilon_0 > 0$, then a constant current $I = \varepsilon/(R_{\text{back}} + R_L + r)$ flows through *0–6–7–8–10*. Bias potential is $\varepsilon_0 = IR_{\text{back}} = \varepsilon R_{\text{back}}/(R_{\text{back}} + R_L + r)$. If the condition $R_{\text{back}} \gg R_L + r$ is met, then $\varphi_0 \approx \varepsilon$.

Let's estimate the equivalent capacitance of the resonator using the formula for the capacitance of a flat capacitor $C = \varepsilon_0 S/l$. With $l = 0.3\,\text{m}$, $S = 0.5\pi r_{\text{wall}}^2 = 8.84 \cdot 10^{-3}\,\text{m}^2$ we find $C = 2.61 \cdot 10^{-13}\,\text{F}$, the capacitance reactance of this capacitor is $X_{0C} = 1/(\omega C) = 249\,\Omega$. Equivalent inductance of the resonator $L = 1/(\omega^2 C) = 1.62 \cdot 10^{-8}\,\text{H}$, inductive reactance $X_L = \omega L = 249\,\Omega$.

We replace the mutual capacitances of the workpiece, which has the shape of a ball of radius $R = 4 \cdot 10^{-3}\,\text{m}$, and the chamber walls with the capacitances of spherical capacitors $C_1 = C_2 = 8\pi\varepsilon_0 R = 8.9 \cdot 10^{-13}\,\text{F}$. Thus, when connected in series, their total capacitance $C_{\text{sum}} = C_1 C_2/(C_1 + C_2) = 4\pi\varepsilon_0 R$ is equal to the capacitance of the ball of radius $R = 4 \cdot 10^{-3}\,\text{m}$. Values of the corresponding capacitance reactances $X_C = 1/(\omega C) = 75\,\Omega$.

1.3. Current-voltage curves of unit and parameters of discharge acceleration zone

The studies, the results of which are presented in this paper, are the continuation of studies started in [29]. Previously, in [29], based on the analysis of current-voltage curves showing the strength of constant current flowing through the nit vs. EMF of the constant voltage source $i(\varepsilon)$, using the relationships found in [32,33], the estimates were obtained for a number of physical parameters characterizing the gas discharge. Values of these parameters: floating potential U_f, electron temperature T_e, ion concentration n_i, average kinetic energy of electrons in the acceleration zone $\bar{\varepsilon}_e^*$ are given in the form of Table 1 [29].

2. Results

2.1. Physical processes occurring in unit

Let us use the equivalent scheme shown in Fig. 2, as well as the current-voltage curve of the unit to analyze the physical processes occurring in it.

The electron current on the current-voltage curve reaches its maximum value at the microwave power level $P_0 = 300\,\text{W}$, the source EMF $\varepsilon \approx +200\,\text{V}$ and amounts to $I_{e0} = 0.02\,\text{A}$, and ion saturation current at the same power is $I_{i0} = 0.01\,\text{A}$. So the relation is $I_{e0}/I_{i0} = 2$. Let us further use the well-known expressions for the electronic saturation current:

$$I_{e0}^* = \frac{1}{4} n_e e S \sqrt{\frac{3k_{\text{B}} T_e}{m_e}}, \qquad (2)$$

and Bohm's formula for the ionic saturation current:

$$I_{i0} = 0.4\, n_i e S \sqrt{\frac{2k_{\text{B}} T_e}{m_i}}. \qquad (3)$$

Here n_e and n_i — electron and ion concentrations, respectively, T_e — electron temperature, m_e and m_i — electron and ion masses, S — surface area of the workpiece, k_{B} — Boltzmann's constant.

From (2) and (3) we find

$$\frac{I_{e0}^*}{I_{i0}} = 0.77 \sqrt{\frac{m_i}{m_e}}. \qquad (4)$$

Substituting into (4) the values of the electron mass and the argon ion mass $m_i = 6.63 \cdot 10^{-26}\,\text{kg}$ at $n_e = n_i$, we find $I_{e0}^*/I_{i0} = k = 210$, which is by more than 100 times greater than value $I_{e0}/I_{i0} = 2$, found from the current-voltage curves. Thus, the workpiece surface is reached by only one out of a hundred electrons generated in the discharge acceleration zone, the rest electrons enter the deceleration zone, and after passing through it they diffuse along with the ions ambipolarly to the walls of the resonator chamber. $I_{e0}^* = 105 I_{e0} = 210 I_{i0}$ flows from the acceleration zone through the deceleration zone. High-energy electrons

Table 1. Discharge parameters determined in [29], using relations obtained in [32,33]

Microwave power P_0 (W)	Floating potential $-U_f$ (V)	Temperature of electrons T_e (K)	Concentration of ions n_i (m^{-3})	Energy of electrons $\bar{\varepsilon}_e^*$ (eV)
32	−130	$6.85 \cdot 10^5$	$1.44 \cdot 10^{15}$	89
119	−140	$1.24 \cdot 10^6$	$1.21 \cdot 10^{16}$	160
172	−130	$1.52 \cdot 10^6$	$1.84 \cdot 10^{16}$	197
225	−118	$1.29 \cdot 10^6$	$2.41 \cdot 10^{16}$	167
275	−85	$7.41 \cdot 10^5$	$2.64 \cdot 10^{16}$	96
300	−35	$4.06 \cdot 10^5$	$6.39 \cdot 10^{16}$	53

accelerated by the microwave field near the surface of the sample in the acceleration zone with distance from it will be decelerated due to inelastic collisions with Ar atoms, transferring them from a normal to an excited electronic state of a discrete or continuous spectrum [27].

Microwave energy entering the resonator chamber from the magnetron is transferred to electrons in the acceleration zone, and with their further movement through the deceleration zone, it dissipates. In the equivalent scheme (Fig. 2) we replace the diffusion current I_{e0}^* with the effective value of the active component $I_R = I_{e0}^*$ of some conduction current I flowing through the resistance R_{forw} of diode VD so that the active power Q_R released at R_{forw} coincides with the intensity of energy loss by electrons in the deceleration zone $Q_R = P_e$.

Let us use the data in Table 1 to estimate the power of electronic energy losses P_e. We will assume that when the electron moves through the deceleration zone, all its energy $\bar{\varepsilon}_e^*$ is lost, then when current I_{e0}^* flows, power is released

$$P_e = \bar{\varepsilon}_e^* I_{e0}^* / e. \tag{5}$$

From (5) for $P_0 = 300$ W we find $P_e = 53 \cdot 2.1 = 111.3$ W. Active power released at R_{forw}:

$$Q_R = P_e = I_R^2 R_{\text{forw}}, \tag{6}$$

where $I_R = I_{e0}^* = 2.1$ A. Hence the resistance of diode VD in Fig. 2 in open mode is $R_{\text{forw}} = P_e / I_R^2 = 111.3/2.1^2 = 25.24\,\Omega$.

For sections *6–7* and *5–9* we use the known relationship connecting total, active and reactive power in during parallel connection:

$$P_0^2 = Q_R^2 + Q_C^2. \tag{7}$$

So, the reactive capacitive power is

$$Q_C = \sqrt{P_0^2 - Q_R^2} = \sqrt{300^2 - 111.3^2} = 278.6\,J,$$

reactive current is $I_C = \sqrt{Q_C / X_C} = \sqrt{278.6/75} = 1.93$ A. From the current-voltage curve of the unit [29] by the slope of the curve to the axis U we find the resistance of the circuit section *0–6–7–10*
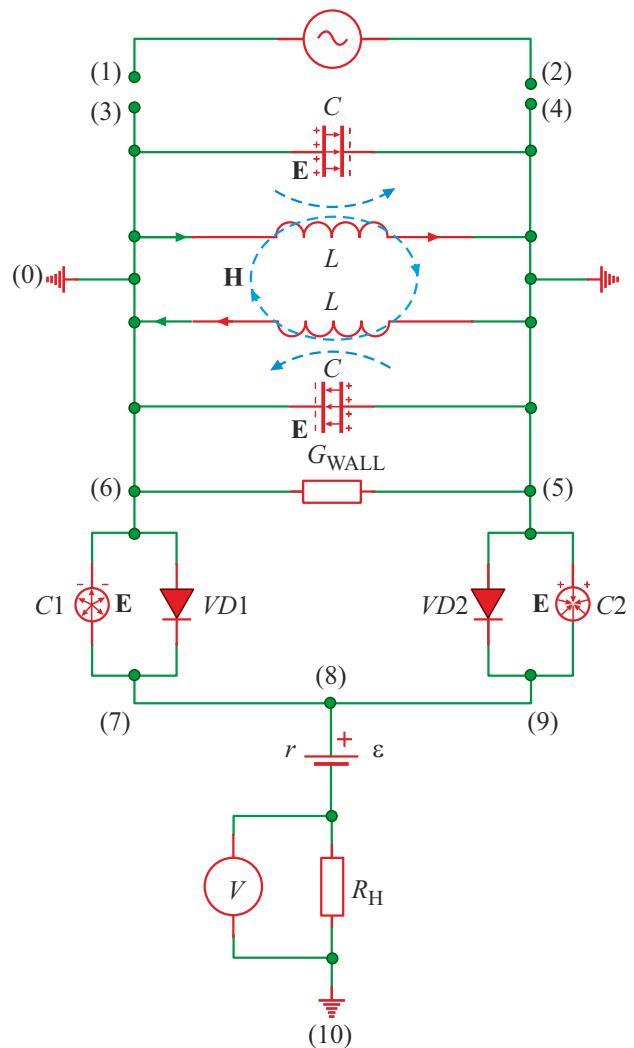
Figure 2. Equivalent scheme of process unit.

$R_{\text{circuit}} = 2.7\,\text{k}\Omega$. Thus, the diode resistance in closed mode is $R_{\text{back}} = R_{\text{circuit}} - r = 2.7 - 1 = 1.7\,\text{k}\Omega$. The effective and amplitude values of the voltage drop across the double layer are $U = I_R R_{\text{forw}} = 2.1 \cdot 25.24 = 53$ V and $U_0 = 75$ V, respectively. It mainly occurs in the discharge acceleration

zone $d = 1.5$ mm wide. The amplitude of the microwave field strength in this zone reaches $E_0 = U_0/d = 5 \cdot 10^4$ V/m. Using the well-known formula [27,34] to estimate the energy acquired by the electron in the microwave field, we obtain

$$\bar{\varepsilon}_e^* = \frac{e^2 E_0^2}{2 m_e \delta_e (\nu_0^2 + \omega^2)}, \qquad (8)$$

where $\delta_e = 0.02$ — average relative fraction of energy transferred by the electron to the atom or molecule in the process of elastic and inelastic collisions with them, ν_0 — frequency of collisions of the electron with gas atoms ($\nu_0 \ll \omega$), m_e — electron mass, ω — magnetron frequency, we find that $\bar{\varepsilon}_e^* \approx 50$ eV, this agrees well with the data in Table 1. Note that the double layer is a half-wave rectifier. The equivalent scheme contains two diodes VD operating in antiphase. Therefore, half of the active power $Q_R = P_e = 111.3$ J will be allocated in the section 6–7, and half — in the section 5–9. Let us now perform similar calculations for the power $P_0 = 172$ W. From the current-voltage curve we find $I_{i0} = 6.3$ mA, the corresponding value $I_{e0}^* = 210 I_{i0} = 1.32$ A. Let us estimate the electron losses using the data in Table 1: $P_e = \bar{\varepsilon}_e^* I_{e0}^*/e = 260$ W, which exceeds $P_0 = 172$ W. A similar situation occurs for $P_0 = 119$ and 225 W. This is possible if the discharge occurs only between the workpiece and one of the ends of the resonator chamber. The workpiece is usually placed at a distance of 10 cm from one and, accordingly, 20 cm from the other end of the resonator. This means that the resistances R_{forw} and R_{back} of one of the diodes, for example, in the section 5–8, should be considered infinite, and energy release occurs in the section 6–7 only. Accordingly, a coefficient of 0.5 appears in the formula for the released electronic power:

$$P_e = Q_R = \bar{\varepsilon}_e^* I_{e0}^*/2e = 130 \text{ W}.$$

Diode resistance in open mode

$$P_{\text{forw}} = P_e/I_R^2 = 130/1.32^2 = 74.61 \,\Omega,$$

reactive power $Q_C = \sqrt{172^2 - 130^2} = 112.6$ J, capacitive current $I_c = \sqrt{Q_C/X_C} = \sqrt{112.6/75} = 1.23$ A. The diode resistance in closed mode is found from the current-voltage curve

$$R_{\text{back}} = R_{\text{circuit}} - r = 66.66 - 1 \approx 65.66 \text{ k}\Omega.$$

Effective value of the voltage drop on the double layer $U = 1.23 \cdot 74.61 = 91.77$ V, amplitude value — $U_0 \approx 130$ V. The amplitude of the microwave field strength in this zone at $d = 1.3$ mm reaches $E_0 = U_0/d = 10^5$ V/m. Using formula (8) we find $\bar{\varepsilon}_e^* = 185$ eV, which agrees well with the data in Table 1.

Table 2 contains the main parameters characterizing the equivalent scheme and its operation at various levels of supplied microwave power: Q_R — active power, Q_C — reactive capacitive power, I_R — effective value of the active component of the current, I_C — effective value

of the reactive component of the current, R_{forw} — diode resistance in open mode, R_{back} — diode resistance in closed mode, E_0 — microwave field strength amplitude near the surface of the workpiece. To complete the picture, let us estimate the losses in the walls of the resonator chamber. From the equivalent scheme (Fig. 2) it is clear that the microwave potential difference is $U_{56} = 2U$, where U — the effective value of the voltage drop across the double layer. For $P_0 = 172$ W, the value is $U = 91.77$ V, and $U_{56} = 2U = 183.54$ V. The characteristic value of the active conductivity of hollow resonators, depending on the specific conductivity of the wall material and the depth of the microwave field penetration into it, is in the range $G = 10^{-4} - 10^{-5} \,\Omega^{-1}$. The power of heat losses in the walls $P_{\text{wall}} = G U_{56}^2 = 0.34 - 3.4$ W is small compared to the power released by electrons in the discharge deceleration zone: $P_{\text{wall}} \ll P_e$.

2.2. Dipole gas discharge in resonator chamber

The nature of the microwave discharge occurring in the resonator chamber significantly depends on the size of the workpiece and its position inside the chamber, which determine the values of electrical capacitances C_1 and C_2 in the equivalent circuit (Fig. 2), as well as the lengths of the discharge gaps between the workpiece and its ends. Typically, during treatment the position of the workpiece is shifted from the axis of the resonator to its side surface so that it is in the electric field of only one of two identical equivalent capacitors C.

If the workpiece in the form of ball is located in the electric field oscillating with amplitude $\mathbf{E}_0$ and frequency ω, at approximately equal distances from the ends, then it receives dipole moment $\mathbf{p}(t)$ oscillating with frequency ω:

$$\mathbf{p} = 4\pi \varepsilon_0 \mathbf{E}_0 R^3 \cos(\omega t + \alpha). \qquad (9)$$

In this case, the charges of the hemispheres change in antiphase with the amplitude $q_0 = C_1 U_0$.

For $P_0 = 275$ W the value is $U_0 \approx 136$ V, from where we find

$$q_0 = 8.9 \cdot 10^{-13} \cdot 136 = 1.21 \cdot 10^{-10} \text{ C}.$$

The oscillation amplitude of the ball's dipole moment is $p_0 = 4/3 q_0 R = 6.45 \cdot 10^{-13}$ C · m. In closed mode, through the diode the following current flows

$$I_{\text{back}} = U/R_{\text{back}} = 96/18.29 \cdot 10^3 = 5.24 \cdot 10^{-3} \text{ A}$$

$$(U = U_0/\sqrt{2})$$

and power is released

$$Q_{\text{back}} = I_{\text{back}}^2 R_{\text{back}} = (5.24 \cdot 10^{-3})^2 19.99 \cdot 10^3 \approx 0.55 \text{ W}.$$

When bias potential $\varphi_0 > 0$ is applied to the workpiece, the height of the potential barrier for electrons existing near its surface decreases. It becomes equal to $(U_f - \varphi_0)e$.

Table 2. Discharge parameters determined based on the analysis of the equivalent scheme of the process unit (Fig. 2)

Microwave power P_0 (W)	Active power $Q_R = P_e$ (W)	Reactive power Q_C (W)	Active current $I_R = I_{e0}^*$ (A)	Reactive current I_C (A)	Resistance of diode in open mode R_{forw} (Ω)	Resistance of diode in closed mode R_{back} (kΩ)	Strength of microwave field E_0 (V/cm)
32	6.5	31.3	0.0735	0.65	1203.20	131.33	$6.9 \cdot 10^4$
119	63.2	100.83	0.79	1.16	101.27	81.06	$9.4 \cdot 10^4$
172	130	112.6	1.32	1.23	74.61	65.66	10^5
225	133.6	181.0	1.6	1.55	52.19	58.30	$9.4 \cdot 10^4$
275	124.8	245.1	1.3	1.80	73.84	19.99	$7.1 \cdot 10^4$
300	111.3	278.6	2.1	1.93	25.24	1.70	$5 \cdot 10^4$

The resistance of the diode R_{back} decreases, and the conductivity of the diode in the closed mode increases. The relationship between the potential φ_0 and the source EMF is determined by Ohm's law $\varphi_0 = \varepsilon / \left(1 + (R_L + r)/R_{back}\right)$. Assuming $R_L = 0$, $r = 1\,\text{k}\Omega$ and determining the value $R_{circuit} \approx 5.49\,\text{k}\Omega$ from the current-voltage curve of the unit for $\varepsilon \approx 65\,\text{V}$, we find $R_{back} \approx 5.49 - 1 = 4.49\,\text{k}\Omega$, $\varphi_0 = 53.16\,\text{V}$. The barrier height is $(U_f - \varphi_0)e = 31.84\,\text{eV}$. For the given value R_{back} we find $I_{back} = U/R_{back} = 96/4.49 \cdot 10^3 = 2.14 \cdot 10^{-2}\,\text{A}$ and the released power $Q_{back} \approx 2\,\text{W}$. At $\varepsilon \approx 65\,\text{V}$, as can be seen from the current-voltage curve of the unit, the constant electronic current $I_e \approx 10\,\text{mA}$ also flows through the workpiece, and power $P_e^* = \bar{\varepsilon}_e^* I_e / e \approx 1\,\text{W}$ is released on the surface. Thus, the useful power is $P_{useful} = Q_{back} + P_e = 2 + 1 = 3\,\text{W}$.

It is obvious that the maximum transfer of electron energy to the workpiece $P_{useful} = I_{e0}^* \bar{\varepsilon}_e^* / 2e \approx 62.4\,\text{W}$ can be achieved by applying the bias potential $\varepsilon_0 = U_f$ to the workpiece, while $R_{back} \approx R_{forw} \approx 74\,\Omega$, however, this requires a constant voltage source with $\varepsilon = U_f(1 + r/R_{back}) \approx 85(1 + 10^3/74) \approx 1.2\,\text{kV}$. It is
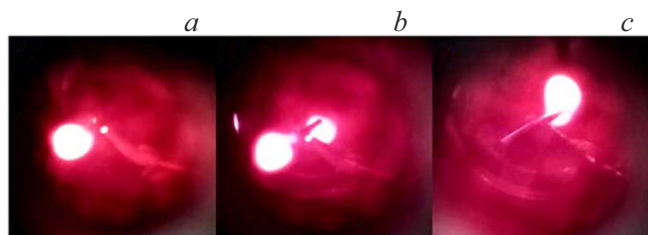
Figure 3. Dipole discharge on the metal rod with a diameter of 6 mm and a length of 95 mm, located at a slight angle to the axis of the resonator chamber in different places relative to its ends: *a* — the discharge is localized only at the end of the rod closer to the observer; *b* — the discharge is localized at both ends of the rod; *c* — the discharge is localized only at the end of the rod, more distant from the observer. The transition from *a* to *b* and further to *c* occurred as the rod was transferred in parallel from the end of the chamber (its door) closest to the observer to the far end.
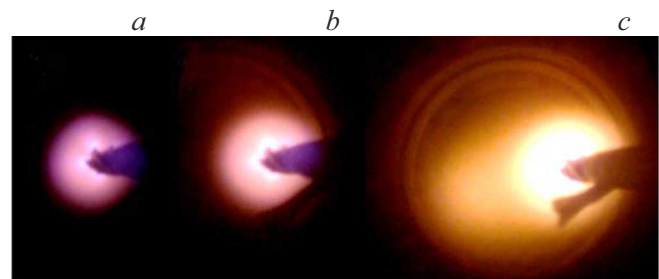
Figure 4. Electric discharge localized on the workpiece near one of the dipole poles, at different levels of supplied microwave power, P_0: *a* — 119, *b* — 225, *c* — 300 W.

convenient to observe various variants of the dipole discharge on the workpiece in the form of a metal rod (Fig. 3). When the workpiece approaches one of the ends of the resonator chamber, the situation may arise when discharge occurs only near one of the poles of the dipole (Fig. 3, 4).

2.3. Structure and parameters of diode layer

A distinctive feature of the microwave discharge is the existence of large stationary electric fields in the near-electrode layer [35].

To estimate the magnitude of the positive charge of the acceleration zone and the magnitude of the electric field strength in it, we will further use Maxwell's equation

$$\text{div}\,\mathbf{E} = \rho/\varepsilon_0 \qquad (10)$$

and the results obtained earlier in [29]. From Table 1 we find that at the level of supplied microwave power is $P_0 = 172\,\text{W}$, which corresponds to the amplitude of the microwave field strength $E_0 = 10^5\,\text{V/m}$ (Table 2), the average ion concentration in the acceleration zone is $n_i = 1.84 \cdot 10^{16}\,\text{m}^{-3}$. Possessing significantly greater mobility $b_e \gg b_i$ than ions, electrons, slowing down, move towards the walls of the resonator chamber faster than ions in the same direction during the diffusion process [36].

For this reason, the concentration of ions in the acceleration zone exceeds the concentration of electrons $n_i > n_e$, and the zone is charged positively. Assuming that the plasma remains quasineutral, i.e., the difference $\Delta n = |n_i - n_e|$ is small compared to n_e and n_i, for further estimates we set $\Delta n \approx 0.1 n_i \approx 1.84 \cdot 10^{15}\,\text{m}^{-3}$. Let us determine from (10) the average electric field strength in the acceleration zone associated with its positive charge

$$E \approx \frac{e \Delta n x}{\varepsilon_0} \approx \frac{1.6 \cdot 10^{-19} \cdot 1.84 \cdot 10^{15} \cdot 1.3 \cdot 10^{-3}}{8.85 \cdot 10^{-12}}$$

$$= 0.43 \cdot 10^5\,\text{V/m}. \tag{11}$$

Here $x = 1.3\,\text{mm}$ — the width of the electron acceleration zone, determined by the size of the purple glow region near the surface of the treated object.

Let us further estimate the positive charge localized in the acceleration zone

$$Q_0 = \frac{4}{3} \pi (R_1^3 - R^3) \Delta n e \approx \frac{4}{3} \pi (5.3^3 - 4^3) \cdot 10^{-9}$$

$$\times 1.84 \cdot 10^{15} \cdot 1.6 \cdot 10^{-19} = 1.04 \cdot 10^{-10}\,\text{C}, \tag{12}$$

where $R_1 = 5.3\,\text{mm}$ — radius of the outer boundary of the acceleration zone, $R = 4\,\text{mm}$ — radius of the workpiece.

Double layer charge located from the center of the ball at distances $R \leq \rho \leq r$

$$Q(r) = \int\limits_R^r 4\pi\rho^2\, w(\rho) d\rho. \tag{13}$$

Here $w(\rho)$ — model function for the electric charge density

$$w(\rho) =$$

$$\begin{cases} A Q_0 (\rho - R)(R_1 - \rho) & \text{on the assumption of } R \leq \rho \leq R_1, \\ -B Q_0 (\rho - R_2)(R_1 - \rho) & \text{on the assumption of } R_1 < \rho \leq R_2, \\ 0 & \text{on the assumption of } R_2 < \rho, \end{cases} \tag{14}$$

where A, B — normalization factors that are selected in such a way that the condition is satisfied

$$\int\limits_R^{R_1} 4\pi\rho^2\, w(\rho) d\rho = Q_0, \quad \int\limits_{R_1}^{R_2} 4\pi\rho^2\, w(\rho) d\rho = -Q_0. \tag{15}$$

Here R_1 — radius of the outer boundary of the acceleration zone, R_2 — radius of the outer boundary of the deceleration zone.

For the power $P_0 = 172\,\text{W}$ we find the value $A \approx 9200\,\text{m}^{-5}$, $B \approx 2350\,\text{m}^{-5}$ the graph of the function $w(\rho)/Q_0$ is shown in Fig. 5, it a. The dependence $h(r) = Q(r)/Q_0$ is shown in Fig. 5, b.

The effective (average over the period) potential energy of the electron in the electric field of the anode zone of the discharge can be written in the form

$$W_{\text{eff}}(r) = -\frac{eC\Delta\varphi}{4\pi\varepsilon_0 r} \exp\left(-\frac{R - r}{r_{\text{D}}}\right)$$

$$- \frac{eQ_0}{4\pi\varepsilon_0 r} \int\limits_R^r 4\pi\rho^2\, w(\rho) \exp\left(\frac{\rho - r}{r_{\text{D}}}\right) d\rho. \tag{16}$$

The first term in (16) determines the potential energy of electron interaction with a charge on the workpiece surface, the second represents the potential energy of electron interaction with positive charge distributed with a volume density $w(\rho)$ in acceleration and deceleration zones of the combined gas discharge. In (16) $C = 4\pi\varepsilon_0 R$ — capacity of the ball, $\Delta\varphi = -U_f + \varphi_0$ — time-averaged potential of the product relative to the plasma, U_f — floating potential value, $r_{\text{D}} = 10^{-5}\,\text{m}$ — Debye radius, $\omega = 1.54 \cdot 10^{10}\,\text{s}^{-1}$, $R = 4 \cdot 10^{-3}\,\text{m}$, $m_e \approx 9.1 \cdot 10^{-31}\,\text{kg}$, $e = 1.6 \cdot 10^{-19}\,\text{C}$. It is obvious that the period averaged value of the microwave potential is $\langle \varphi_{\text{UHF}} \rangle = 0$. The dependence $W_{\text{eff}}(r)$, plotted in MATHCAD, is presented in Fig. 6.

From Fig. 6 it is clear that when positive bias potential φ_0 is applied to the workpiece, the height of the potential barrier for electrons existing near the surface of the workpiece decreases, which leads to a decrease in the resistance of the diode layer VD in closed mode R_{back}.

3. Discussion

To estimate the value of the field strength E_0 in the resonator chamber, we use the relations

$$W = \frac{\varepsilon_0 E_0^2}{2} V = \frac{P_0 Q_0}{\omega}, \quad E_0 = \left(\frac{2P_0 Q_0}{\varepsilon_0 V \omega}\right)^{1/2}. \tag{17}$$

Here W — time-average value of electromagnetic energy stored in the resonator, Q_0 — resonator quality factor, V — resonator volume, P_0 — power delivered by the magnetron, ω — cyclic frequency. From (17) for the parameter values $P_0 = 28\,\text{W}$, $V = 5 \cdot 10^{-3}\,\text{m}^3$, $Q_0 = 1.2 \cdot 10^5$, $\omega = 1.54 \cdot 10^{10}\,\text{s}^{-1}$ we find Thus, the value E_0 reaches the microwave breakdown threshold $E_0 = E_{\text{Cr}} = 10^5\,\text{V/m}$ of argon, which depends on pressure, frequency and discharge volume, after which a dark discharge occurs with small current up to $10^{-5}\,\text{A}$. For gas the breakdown means transition to an ionized state. When the level of supplied microwave power increases to $P_0 = 32\,\text{W}$, a glow appears near the workpiece surface. The current flowing through the discharge plasma, the concentration of ions and electrons and conductivity increase, and the electric field strength required to maintain the given current is $E_0 = 6.9 \cdot 10^4\,\text{V/m} < E_{\text{Cr}}$. After ignition of the microwave discharge the energy stored in the resonator decreases. The field E_0 is usually less than E_{Cr} (Table 2), which is due to
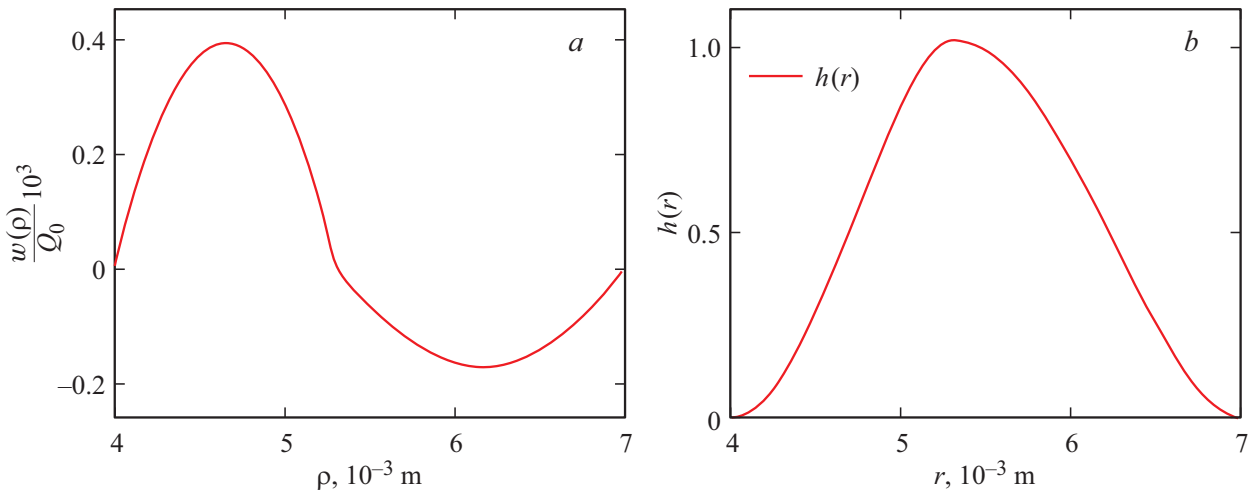
Figure 5. Electric charge distribution in the near-electrode region of the discharge: $4 \cdot 10^{-3}$ m $< \rho < 5.3 \cdot 10^{-3}$ m — positively charged acceleration zone, $5.3 \cdot 10^{-3}$ m $< \rho < 7 \cdot 10^{-3}$ m — negatively charged deceleration zone.
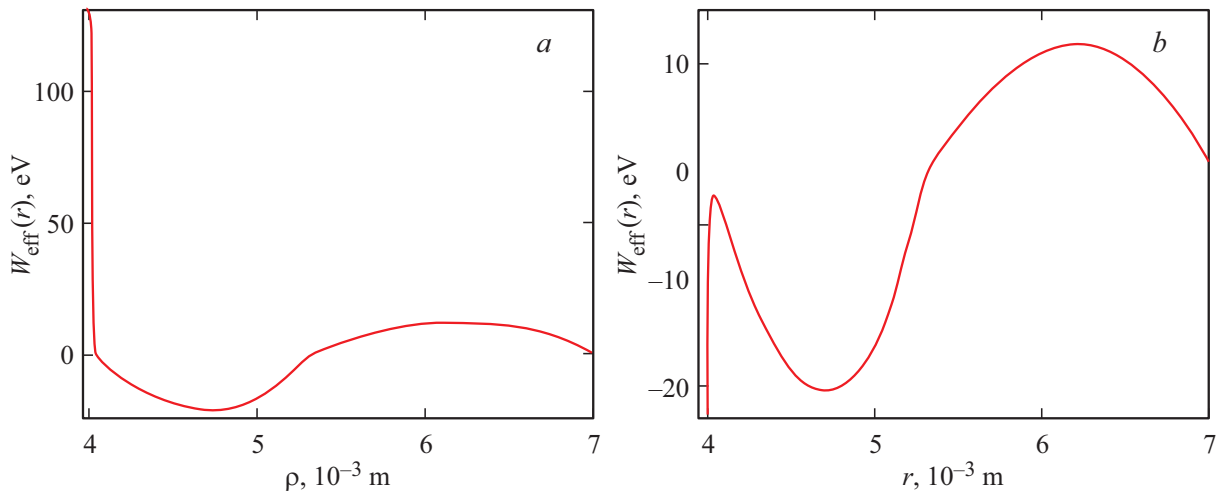
Figure 6. Dependence $U_{\text{eff}}(r)$ at microwave power level $P_0 = 172$ W: a — $\Delta\varphi = -U_f = -130$ V, $\varphi_0 = 0$;b — $\Delta\varphi = -U_f + \varphi_0 = -130$ V $+ 153$ V $= 23$ V, $\varphi_0 = 153$ V.

a number of reasons, including the presence in the plasma of the formed discharge of a significant concentration of excited atoms, as a result of which in the process of the discharge maintenance the role of stepwise ionization and heating of electrons due to the energy of metastable atoms becomes essential.

Note that the largest value of the active component of the current flowing through the unit $I_R = 2.1$ A, according to Table 2, is achieved at the highest value of the supplied microwave power $P_0 = 300$ W, which corresponds to the smallest value of the microwave field strength amplitude $E_0 = 5 \cdot 10^4$ V/m near the surface of the workpiece. From Table 1 it is clear that a given level of microwave power corresponds to the highest concentration of charged particles in the discharge plasma $n_i = 6.39 \cdot 10^{16}$ m^{-3} and the lowest electron energy $\bar{\varepsilon}_e^* = 53$ eV.

As P_0 increases, the appearance of the discharge changes significantly. At a low level of microwave power a clear difference is visible between the acceleration zone and the deceleration zone of electrons (Fig. 4, a, b). The deceleration zone is purple. As P_0 increases, the radius of the plasma cloud increases, the visual distinction between the acceleration and deceleration zones disappears, and the color of the cloud becomes red-orange. All this indicates both increase in the electron concentration and decrease in their energy (Fig. 4, c).

The optimal level of supplied microwave power for workpiece treatment obviously depends on the workpiece material and its geometric dimensions and, as can be seen from Tables 1 and 2, lies in the range $P_0 \sim 100-250$ W. At low powers $P_0 < 100$ W too little active power is released in the chamber Q_R, and at high powers $P_0 > 250$ W with P_0 increasing the share of active power Q_R/P_0 decreases, and

the share of reactive power Q_C/P_0 increases, which leads to instability of the magnetron and decrease in the unit efficiency. Also, with value P_0 increasing there is decrease in the average kinetic energy of electrons accelerated by the microwave field and arriving at the workpiece surface.

The diode properties of the double layer depend significantly on the bias potential applied to it φ_0. With an increase in the positive value φ_0, the height of the potential barrier for electrons eU_f that exists near the surface of the workpiece decreases and, accordingly, the resistance R_{back} of the diode in closed operating mode decreases. When the barrier completely disappears, for which it is necessary to apply potential $\varphi_0 = U_f$ to the workpiece, dissipation up to $10-20\%$ of the active power released in the unit is possible, which contributes to surface heating up to the melting point. Ions falling on the surface diffuse into the volume, forming a hardened surface layer.

Parameters used for workpieces treatment in the electronic current unit: $j_e \sim 5-40\,\mathrm{mA/cm^2}$, $\bar{\varepsilon}_e^* \sim 50-200\,\mathrm{eV}$ at energy flux density $\sim 1-4\,\mathrm{W/cm^2}$ and ion currents $j_i \sim 2-5\,\mathrm{mA/cm^2}$, $\bar{\varepsilon}_i^* \sim 50-100\,\mathrm{eV}$. These values are very close in value to the parameters of electron and ion beams: $j_e \sim 10-30\,\mathrm{mA/cm^2}$, $\bar{\varepsilon}_e^* \sim 50-100\,\mathrm{eV}$ at energy flux density $\sim 3-5\,\mathrm{W/cm^2}$, $j_i \sim 1-7\,\mathrm{mA/cm^2}$, $\bar{\varepsilon}_i^* \sim 100-300\,\mathrm{eV}$ used in the unit described in [37]. The difference lies in the characteristic dimensions of the treated workpieces. The installation shown in Fig 2 is designed to treat small workpieces with surface area up to $20\,\mathrm{cm^2}$ with power consumption up to $1\,\mathrm{kW}$, and in the unit developed by the authors [37] It is advisable to treat large workpieces with surface area of up to $2000\,\mathrm{cm^2}$, since power of tens of kW is consumed to create the electron beam.

The glow of the dipole discharge plasma is unevenly distributed along the workpiece surface. Near the dipole poles the energy density of the microwave discharge reaches its maximum values, and the plasma has the greatest effect on the workpiece surface. In the middle of the rod, where the intensity of the plasma glow is low or there is no glow at all, the workpiece surface is treated to a lesser extent.

If in the region of the dipole discharge pole the workpiece surface has a complex relief, then the microwave field strength lines are concentrated near areas with the greatest positive curvature (convexities), where the surface electric charge density is maximum σ, and, consequently, $E_0 = \sigma/\varepsilon_0$, the energy $\bar{\varepsilon}_e^* \sim E_0^2$ acquired by the electron in the microwave field (8), as well as the plasma glow intensity reach their maximum values. Just in these areas the largest number of high-energy electrons accelerated by the microwave field falls per unit surface area of the workpiece per time unit, resulting in more intense heating, which leads to the most active process of thermal diffusion of positive ions of the process gas inside the sample. For example, when treating metal-cutting tools, maximum surface hardening occurs near their cutting edges. Due to the increased energy density of the microwave field $w \sim E_0^2$ near such surface areas with microwave discharge power of only $0.03-0.3\,\mathrm{kW}$, a high growth rate of the thickness of the

hardened layer $0.4\,\mu\,\mathrm{m/min}$ is achieved. The usual treatment time for the workpiece does not exceed $10-12\,\mathrm{min}$.

For comparison, note that in the ARDIS-100 unit, developed at the General Physics Institute of the Russian Academy of Sciences, it is possible to deposit hardening diamond coatings on flat or cylindrical substrates only. The main element of the unit is the microwave resonator. The resonator is manufactured in such a way that the maximum energy release in the microwave discharge is achieved near the substrate. The growth rate of the thickness of the diamond layer is $1.75\,\mu\mathrm{m/min}$ at a microwave discharge power of $3\,\mathrm{kW}$ [14,38,39], plasma-forming gas pressure (20% Ar, 15% CH_4, 65% H_2) $13\,000-27\,000\,\mathrm{Pa}$. A similar method of generating the microwave discharge for the diamond films deposition is also presented in a number of other papers, however, the growth rate of the diamond coating in them is much lower — $< 0.2\,\mu\mathrm{m/min}$, and the microwave discharge power reaches $8\,\mathrm{kW}$, which is significantly higher than in ARDIS-100 [40–42]. For diamond treatment of small-sized workpieces, the method of diamond film deposition from the plasma of microwave torch at atmospheric pressure can be used. The torch method [14] allows you to apply a diamond coating to the surface of objects of arbitrary shape due to the use of object scanning devices above the torch. The work[piece temperature is maintained by an additional heat source.

Conclusion

Thus, the following results were obtained in the paper:

1. It is shown that near the workpiece surface a double layer appears, formed by acceleration and deceleration zones of the gas discharge, which has diode properties. In the open mode, when the workpiece potential is lower than the floating potential, the „diode" lets in fast electrons from the acceleration zone to the deceleration zone and has a relatively low resistance. The decrease in fast electrons in this region is constantly replenished due to the acceleration of slow electrons in the high-frequency electric field of the microwave discharge. The low throughput capacity of the „diode" in the closed mode is associated with the presence of a negative floating potential on the workpiece, which leads to the existence in the near-surface layer of the discharge of the potential barrier with height $35-140\,\mathrm{eV}$, that does not allow electrons with lower energy to approach the surface, while electrons with larger energy create negative current compensating the current of positive ions. When workpiece potential exceeds the floating potential, the resistance of the „diode" is high a small electron current flows through the „diode" slightly exceeding the ionic saturation current.

2. The height of the potential barrier can be adjusted by applying a constant bias potential to the workpiece. When positive bias potential is applied, the barrier height decreases, which leads to a decrease in the resistance of the diode layer in the closed mode and, accordingly, to

an increase in the influx of fast electrons to the workpiece surface, heating it to high temperature from $500°C$ up to the melting point, making possible the thermal diffusion of ions inside the workpiece volume. Thus, there is a significant analogy between the action of combined gas discharge plasma on the workpiece surface and the action of electron beam passing through the plasma. In both cases the heating of the product occurs primarily due to the electron energy transferred to it.

3. The increase in the microwave power supplied from the magnetron to the resonator chamber causes an increase in the effective values of the active and reactive components of the currents flowing through the unit, reactive capacitive power, as well as the concentrations of electrons and ions in the gas discharge plasma. The resistance values of the diode layer in open and closed modes decrease. Such parameters as the active power released in the discharge deceleration zone, the average kinetic energy of electrons in the discharge acceleration zone, the amplitude of the electric field strength near the workpiece surface reach their maximum values in the power range $P_0 \sim 100-250\,\mathrm{W}$, which is most suitable for workpieces treatment. The specific value of the optimal power for treatment, of course, depends on the material, size and shape of the workpiece.

4. The workpiece located in the microwave field acquires a dipole moment that oscillates with the field frequency. The position inside the resonator chamber, the size and shape of the workpiece determine the values of its mutual capacitances with the ends of the chamber, which, in turn, determine the nature of the resulting dipole discharge. At the same or similar values of capacitances, which corresponds to location near the center of the chamber, the plasma glow is localized near both poles of the dipole. If you move the workpiece towards one of the ends, the glow is localized at one of its poles only.

Funding

Conflict of interest

The authors declare that they have no conflict of interest.

References

[1] V.K. Sheleg, A.N. Zhigalov, D.D. Bogdan. Nauka i tekhnik, **19** (4), 271, (2020). (in Russian)

[2] S. Hussain, X. Yang, M.K. Aslam, A. Shaheen, M.S. Javed, N. Aslam, B. Aslam, G. Liu, G. Qiao. Chem. Engineer. J., **391**, 123595 (2020).

[3] L. Luis, J. Andrade, C.M. Pesqueira, I. Siqueira, G.B. Sucharski, M.J. de Sousa. J. Thermal Spray Technol., **30**, 205 (2021). DOI: 10.1007/s11666-021-01152-8

[4] A. Mosavi, F. Salehi, L. Nadai, S. Karoly, N.E. Gorji. Results in Physics, **16**, 102883 (2020). DOI: 10.1016/j.rinp.2019.102883

[5] V.E. Gromov, Yu.F. Ivanov, S.V. Konovalov, Yu. Feng, D.A. Kosinov. Vestnik MGTU im. G.I. Nosova, **14** (2), 69 (2016). (in Russian)

[6] S.N. Grigoriev, A.S. Metel, T.V. Tarasova, A.A. Filatova, S.K. Sundukov, M.A. Volosova, A.A. Okunkova, Yu.A. Melnik, P.A. Podrabinnik. Metals, **10** (11), 1540 (2020).

[7] V.A. Aleksandrov, L.G. Petrova, A.S. Sergeeva, V.D. Aleksandrov, E.U. Akhmetzhanova. Russ. Engineer. Res., **39** (8), 693 (2019).

[8] N.V. Gavrilov, A.S. Mamaev, A.V. Chukin. Poverkhnost'. Rentgenovskie, sinkhrotronnye i nejtronnye issledovaniya, **11**, 61 (2017). (in Russian).

[9] S. Grigoriev, A. Metel, M. Volosova, Y. Melnik, H.A. Ney, E. Mustafaev. Technologies, **7** (3), 62 (2019). DOI: 10.3390/technologies7030062

[10] M. Ueda, C. Silva, B. Gelson, L. Pichon, H. Reuther. J. Vacuum Sci. Technol. B, **37**, 042902 (2019). DOI: 10.1116/1.5092435

[11] L. Luiz, B.C.E.S. Kurelo, G.B. de Souza, J. de Andrade, C.E.B. Marino. Mater. Today Commun., **28**, 102655 (2021). DOI: 10.1016/j.mtcomm.2021.102655

[12] B. Yang, Q. Shen, Z. Gan, S. Liu. Cryst. Eng. Comm., **21**, 6574 (2019).

[13] K.F. Sergeychev, N.A.Lukina, N.R. Arutyunyan. Fizika plazmy, **45** (6), 513 (2019) (in Russian).

[14] K.F. Sergejchev. Uspekhi prikladnoi fiziki, **3** (4), 342 (2015). (in Russian).

[15] N.V. Gavrilov, A.S. Mamaev, A.V. Chukin, J. Surf. Invest., **11**, 1167 (2017).

[16] V.A. Shabashov, N.V. Gavrilov, K.A. Kozlov, A.V. Makarova, S.G. Titova, V.I. Voronin. Fizika metallov i metallovedenie, **119** (8), 802 (2018). (in Russian)

[17] V.A. Burdovitsin, D.A. Golosov, E.M. Oks, A.V. Tyunkov, Y.G. Yushkov, D.B. Zolotukhin, S.M. Zavadsky, Surf. Coat. Technol., **358**, 726 (2019).

[18] N.N. Koval, A.I. Ryabchikov, D.O. Sivin, I.V. Lopatin, O.V. Krysina, Y.H. Akhmadeev, D.Y. Ignatov, Surf. Coat. Technol., **340**, 152 (2018).

[19] T. Moskalioviene, A. Galdikas. Surf. Coatings Technol., **366**, 277 (2019).

[20] A.S. Metel, S.N. Grigoriev, M.A. Volosova, Yu.A. Melnik, E.S. Mustafaev. Instruments and Experimental Techniques, **65** (6), 910 (2022).

[21] W. De Oliveira, B. Kurelo, D. Ditzel, F. Serbena, C. Foerster, G. de Souza. Appl. Surf. Sci., **434**, 1161 (2018).

[22] K. Norrman, Y. Wang, E. Stamate, W. Zhang. Heliyon, **5**, e01943 (2019).

[23] W.R. de Oliveira, A.R. Mayer, G.B. de Sousa, H.D. Carvajal Fals, A.G.M. Pukasiewicz. J. Thermal Spray Technol., **32**, 737 (2023).

[24] V.P. Budaev, S.D. Fedorovich, A.V. Lubenchenko, A.V. Karpov, N.E. Belova, M.K. Gubkin. Heliyon, **6**, e05510 (2020).

[25] M.S. Stechyshyn, A.V. Martynyuk, Y.M. Bilyk, V.P. Oleksandrenko, N.M. Stechyshyna. Mater. Sci., **53**, 343 (2017).

[26] B. Brzhozovskii, M. Brovkova, S. Gestrin, V. Martynov, E. Zinina. J. Phys. D: Appl. Phys., **51**, 145204 (2018).

[27] B. Brzhozovskii, M. Brovkova, S. Gestrin, V. Martynov, E. Zinina J. Phys. D: Appl. Phys., **52**, 485202 (2019)

[28] B.M. Brzhozovsky, S.G. Gestrin, E.P. Zinina, V.V. Martynov. ZhTF, **87** (12), 1857 (2017). (in Russian)

[29] B. Brzhozovskii, M. Brovkova, S. Gestrin, E. Zinina, V. Martynov. Heliyon, **7**, e07006 (2021).

[30] X. Deng, Y. Takaoka, H. Kousaka, N. Umehara. Surf. Coating. Technol., **238**, 80 (2014).

[31] L.J. Zhu, Z.Q. Chen, Z.X. Yin, G.D. Wang, G.Q. Xia, Y.L. Hu, X.L. Zheng, M.R. Zhou, M. Chen, M.H. Liu. Chinese Phys. Lett., **31**, 035203 (2014).

[32] Ya.I. Londer, K.N. Ulyanov. High Temp., **51** (1), 7 (2013).

[33] Ya.I. Londer, K.N. Ulyanov. High Temp., **52** (6), 787 (2014).

[34] U.P. Raizer. UFN, **132** (3), 549 (1980) (in Russian).

[35] V.I. Farenik. Phys. Surf. Eng., **2** (1), 117 (2004).

[36] E.M. Lifshitz, L.P. Pitaevskiy. *Teoreticheskaya fizika. X. Fizicheskaya kinetika* (Nauka, M., 1979) (in Russian)

[37] N.V. Gavrilov, A.I. Menshakov. Pribory i tekhnika eksperimenta **5**, 140 (2011).(in Russian).

[38] A.K. Rebrov, M.V. Isupov, A.Yu. Litvintsev, V.F. Burov. Prikladnaya mekhanika i tekhnicheskaya fisika, **59** (5), 5 (2018). (in Russian).

[39] A. Popovich, M. Shevchenko, S. Savin, E. Zavedeev, M. Zanaveskin, A. Sinogeykin, V. Ralchenko, V. Konov. Coatings, **10** (10), 939 (2020). DOI: 10.3390/coatings10100939

[40] K. An, S.W. Yu, X.J. Li, Y.Y. Shen, B. Zhou, G.J. Zhang, X.P. Liu. Vacuum, **117**, 112 (2015). DOI: 10.1063/6.0000846

[41] C.J. Widmann, W. Muller-Sebert, N. Lang, C.E. Nebel. Diamond Related Mater., **64**, 1 (2016).

[42] J. Weng, F. Liu, L.W. Xiong, J.H. Wang, Q. Sun. Vacuum, **147**, 134 (2018).

Translated by I.Mazurov